



## Full Text View

[Volume 29, Issue 6 \(June 1999\)](#)

## Journal of Physical Oceanography

 Article: pp. 1085–1095 | [Abstract](#) | [PDF \(184K\)](#)

## On Internal Wave Groups

S. A. Thorpe

*Department of Oceanography, Southampton Oceanography Centre, Southampton, United Kingdom*

(Manuscript received January 20, 1998, in final form May 20, 1998)

DOI: 10.1175/1520-0485(1999)029&lt;1085:OIWG&gt;2.0.CO;2

## ABSTRACT

The pattern of disturbance left by internal wave groups traveling in a uniformly stratified ocean is examined. Particular attention is given to the temporal and spatial reoccurrence of extreme values of some parameter  $Q$ , such as the Richardson number or the wave slope, which may determine, for example, the onset of wave breaking in the group or the wave group's refraction of smaller-scale waves. Extreme values reoccur with a period  $T$ , equal to the period of the internal waves, and are sustained along a direction that depends on the wave frequency, but that, over much of the frequency range from  $f$  (the Coriolis frequency) to  $N$  (the constant buoyancy frequency) of the internal waves, is nearly horizontal. The size of regions in which extreme values are achieved depends on the aspect ratio of the region of a wave group, termed the "group breaking region,"  $V$ , within which values of  $Q$  exceed some threshold  $Q_c$ .

Conditions in which regions of past exceedence of  $Q_c$  ("scars" left by waves in passing wave groups) overlap, so as to be always observed by vertical or horizontal profile measurements, depends on the ratio  $\tau/T$ , where  $\tau$  is the time for which  $Q > Q_c$  as a wave passes through  $V$ . Near-inertial and semidiurnal tidal internal waves are more likely to leave overlapping scars and may lead to more general mixing of the ocean than, for example, internal wave groups generated by tidal flow over small horizontal scale (1–3 km) topography. It is suggested that wave groups may be evident, and consequently their effects in promoting turbulence may be largest, near the site of internal wave generation, just where recent observations suggest is the region of enhanced turbulent dissipation in the abyssal ocean.

## Table of Contents:

- [Introduction](#)
- [Groups of internal inertial](#)
- [Discussion](#)
- [Conclusions](#)
- [REFERENCES](#)
- [TABLES](#)
- [FIGURES](#)

## Options:

- [Create Reference](#)
- [Email this Article](#)
- [Add to MyArchive](#)
- [Search AMS Glossary](#)

## Search CrossRef for:

- [Articles Citing This Article](#)

## Search Google Scholar for:

- [S. A. Thorpe](#)

## 1. Introduction

One of the most powerful, and yet elementary, concepts basic to the understanding of the physical properties of waves is

that of wave energy traveling in groups of waves at the group velocity. It provides a quite accurate means of predicting the time interval between the breaking of surface gravity waves in a local region of the sea surface in deep water ([Farmer and Vagel 1988](#)) or, more generally, the interval between the reoccurrence of extremes, such as high waves, large accelerations, or large wave-induced particle speeds, as waves advance in a wave group. The interval is approximately  $2T$ , where  $T$  is the wave period ([Donelan et al. 1972](#)). The explanation is simple: from the linear form of the dispersion relation,  $\sigma^2 = gk$ , where  $\sigma$  is the wave frequency and  $k$  the wavenumber, it follows that the phase speed of the waves,  $\mathbf{c} = \sigma/k$ , is twice the group speed,  $\mathbf{c}_g = \partial\sigma/\partial k$ . The time needed for a wave to advance by one wavelength,  $\lambda$ , through the advancing group to reach the position in the group at which its predecessor began to break (and where it too will reach its breaking point) is  $\lambda/(\mathbf{c} - \mathbf{c}_g)$  or  $2\lambda/T$ , which, since  $\mathbf{c} = \lambda/T$ , is equal to  $2T$ . For simplicity, it is assumed that the group is steady, with breaking setting in at the same position in the group as it advances, and that the phase speed of waves does not change as the waves pass through the group. The associated assumption that the linear dispersion relation is valid is an approximation, but one which is accurate to about 10% (see [Longuet-Higgins 1975](#)). The location of the breaking, or extreme value, moves forward with a wave crest at the phase speed that, for surface gravity waves, happens to be in the same direction as the group velocity. The position at which one wave eventually ceases to break will be within the area in which its successor breaks if the duration of breaking  $\tau$ , the time for which a wave continues to break while advancing at its phase speed, is greater than the wave period  $T$ . The condition,  $\tau > T$ , is also necessary for the foam patch of one wave to overlap in space with that of its neighboring breaking wave, but it is also necessary that the foam *persists* for at least a time  $2T - \tau$  if foam left by one wave is to last until its successor begins to break, thus forming a continuous foam patch. Some of these ideas are shown graphically in [Fig. 1](#). They are simplistic, supposing that a wave group is steady, which has implications for its energy supply and loss, but provide useful results or predictions that can be compared with observations.

Relations between the occurrence of breaking waves in photographs of the sea surface and of measurements of waves breaking at fixed positions can also be derived ([Thorpe and Humphries 1980](#)). The number of waves measured as a wave group passes a fixed position is *twice* that actually in the group (e.g., the number that could be counted in a photograph); if there are  $n$  waves in the group, the time to pass is  $n\lambda/\mathbf{c}_g = 2n\lambda/\mathbf{c} = 2nT$ , but each wave takes a time  $T$ , so the number of waves measured is  $2n$ . [In water of finite depth  $h$ , where the dispersion relation becomes  $\sigma^2 = gk \tanh kh$  and hence  $\frac{1}{2} < \mathbf{c}_g/\mathbf{c} < 1$ , the time taken for  $n$  waves to pass is  $n\lambda/\mathbf{c}_g = nT/(\mathbf{c}_g/\mathbf{c})$ , which lies between  $nT$  and  $2nT$ ; the number of waves measured at a fixed point is between  $n$  and  $2n$ .] The presence of wave groups has therefore some effect on the interpretation of properties of wave amplitude recorded in different ways (e.g., by stationary or rapidly moving sensors to which the photograph more closely corresponds) and may also be important in the assessment of the impact (i.e., number of high waves and forces) of waves on fixed structures.

Given the power of these ideas, it is remarkable that relatively little attention has been given to the presence and consequence of *internal* gravity wave groups in the ocean; there appears to be no study of their properties that matches that of surface waves (e.g., see [Trulsen 1989](#); Banner and Tian, manuscript submitted to *J. Fluid Mech.* and references therein). It is particularly surprising because of the association, noted above, between wave groups and wave breaking (which might, for example, dictate the optimum strategy to *measure* the waves and their breaking) and because, following [Munk's \(1966\)](#) paper on diapycnal diffusion, a large part of the motivation for the study of internal waves has been to assess their role in ocean mixing. Knowledge of the statistics of extreme events in the internal wave field is sparse in spite of their importance in estimating dispersion or even large transient currents, which might, for example, be applicable to predicting forces on offshore structures. Such quantities as mean-square isopycnal slope and mean-square shear can be derived from the internal wave spectrum ([Garrett and Munk 1972](#)). Richardson number statistics may also be derived ([Desaubies and Smith 1982](#)), although consequent diapycnal diffusion is very uncertain. Direct recordings of currents and temperature fluctuations have been collected for many years and measurements of the Richardson number are now becoming more frequent (e.g., see [Simpson 1972](#); [Evans 1982](#); [Eriksen 1978](#); [Padman and Jones 1985](#); [Kunze et al. 1990](#)), but a study of the spatial distribution, movement, and reoccurrence of parameters that might characterize the onset of mixing within the field of internal waves, and so elucidate its physical origin, is still lacking.

The slope of the frequency spectrum of internal waves is close to  $-2$  ([Garrett and Munk 1975](#); [Munk 1981](#)), while that of surface waves beyond the spectral peak is about  $-4$  to  $-5$  ([Phillips 1966](#)). Dominant waves in the internal wave spectrum are less pronounced than are surface waves except perhaps at tidal or inertial frequencies, and groups are less readily detected. Internal wave "swell" from distant storms has not been identified (but see later reference in this section to the radiation of baroclinic tides), and the group structure commonly seen in surface wave swell is rarely reported in observations of internal waves of moderate frequency. Early studies of internal waves did, however, point to the presence of groups (e.g., [Sabinin 1973](#); [Brekhovskikh et al. 1975](#); [Käse and Siedler 1980](#)), but mainly those of the first mode traveling horizontally on the seasonal thermocline where their properties are akin to those of surface waves, the vector phase speed  $\mathbf{c}$  and group velocity  $\mathbf{c}_g$ , being *parallel*. Some of the observed internal waves groups were possibly soliton packets associated with a propagating change in thermocline depth (e.g., see [Apel et al. 1985](#); [Fedorov and Ginsberg 1986](#); [Ostrovski and Stepanyants 1989](#)) and, hence, are more akin to undular bores or hydraulic jumps described by the surface gravity wave shallow water theory than to surface wave groups in deep water.

In uniformly stratified water the phase velocity  $c$  and group velocity  $c_g$  of internal waves are normal to one another and, as described in [section 2](#), the simple ideas of group behavior derived from surface wave groups do not carry over. Inertial gravity wave groups propagate with nonzero vertical components of group velocity. Evidence of upward phase propagation and downward group propagation, indicating a surface source for the inertial waves, comes from velocity profilers ([Leaman and Sanford 1975](#)) and Doppler sonar studies ([Pinkel 1983](#)). The observations of phase propagation are consistent with the predicted behavior of a group of inertial waves traveling downward. Numerous other observations of near-inertial wave groups have been reported, for example, by [Pollard and Millard \(1970\)](#), [Mied et al. \(1987\)](#), and [Smyth et al. \(1996\)](#).

These observations of near-inertial waves suggest that the groups contain some 3–7 waves. In [Mowbray and Rarity's \(1967\)](#) laboratory experiments demonstrating the propagation of internal waves along group characteristics from an oscillating cylinder, the width of the paths or “rays” is only about twice the wavelength, that is, two waves in the wave group; short groups are physically possible. Observational evidence that internal waves in the deep ocean generally propagate along raylike paths at an angle to the horizontal, like those in the laboratory experiments, is however meager. The clearest evidence comes from observations of internal tidal waves generated by the interaction of the baroclinic tides with the topography in local regions at, or near, the shelf break in the Bay of Biscay. The waves have been traced along ray characteristics from the shelf break to the bottom of the bay at depths of 3.8 km ([Pingree and New 1989](#); see also [New 1988](#)). There is even evidence of their reflection at the seabed and return, again following ray characteristics, to the upper ocean ([New and Pingree 1990, 1992](#)). Further evidence of internal tidal ray propagation is discussed by [Levine et al. \(1983\)](#), and recent interest in the subject has been aroused by observations by [Dushaw et al. \(1995\)](#), showing that internal tidal waves propagate some 2000 km from a source in the Hawaiian Islands (see also [Ray and Mitchum 1996](#)).

Observations by [Marmorino \(1987\)](#) and [Marmorino et al. \(1987\)](#), using towed thermistor arrays, identify the presence of groups of 4–10 small-scale internal waves, sometimes with vertical scales less than a wavelength in extent, within the seasonal thermocline. Their measurements also provided evidence for the existence of the groups of near-inertial waves, within which are the mixing *patches* with vertical scale of order 10 m, reported by [Gregg et al. \(1986\)](#). Gregg et al. also identify *puffs*, short-lived events ( $<N^{-1}$  in lifetime and with horizontal scales  $<a$  few 100 m) thought to be associated with internal gravity waves. The patches have horizontal scales of several kilometers and are often tilted to the horizontal, with temperature changing along their length and with evident signs of upward vertical migration in time. [Pinkel et al. \(1991\)](#) describe the analysis of 10 000 CTD profiles made from *FLIP* over a period of 20 days in PATCHEX and, in particular, examine the properties of the strain field. The 20-m strain field is dominated by inertial and  $M_2$  tidal motions. In the 2-m strain field “lenses” of low density are found that sometimes persist for up to 8 h and propagate vertically with respect to the density field over tens of meters.

Groups of short internal waves at depths of 200–350 m in the ocean thermocline have recently been observed from *FLIP* in water some 1 km deep by Alford and Pinkel (manuscript submitted to *J. Geophys. Res.*). Statically unstable overturns occur preferentially within the wave groups, particularly those having downward group velocity, suggesting a surface source.

One condition that may favor the occurrence of wave groups is that the generation processes are intermittent, or at least unsteady. This will generally be the case for internal waves ([Thorpe 1974](#)). Even the rhythmic generation by topography–barotropic tide interaction is subject to spring–neap, if not diurnal, variations. A further contributing property is that regular internal wave trains become unstable ([Borisenko et al. 1976](#); [Thorpe 1977](#)). The photograph shown by [Benjamin \(1967\)](#) is a graphic illustration of the breakdown of a regular surface gravity wave train into irregular short wave groups. A further contributor is that internal waves strongly interact with each other ([Phillips 1966](#); [Martin et al. 1972](#)). It is possible that this property, occurring at second order between triads of waves, has a greater effect on the development and stability of internal wave groups than it does for surface waves, where four waves are generally needed for interaction ([Phillips 1960](#); [Hasselmann 1962](#); [Longuet-Higgins 1962](#)). Other factors, such as parametric instability, critical layers, wave caustics, and wave–wave interaction, may also contribute to the occurrence of groups, as well as to the propagation and breaking of wave packets ([Henyey and Pomphrey 1983](#); [Broutman and Grimshaw 1988](#); [Winters and D'Asaro 1992](#)). Perhaps the relatively sparse attention given to internal wave groups is due to a supposition that, unlike surface wave groups, which may be continually forced by the wind (although a robust theoretical discussion of wave *group* generation by wind is yet to be developed), internal wave groups will soon interact, change their form, or disintegrate as they leave and propagate away from their localized energy and momentum sources. It is, however, in regions close to viable sources of internal waves that enhanced diapycnal mixing occurs in the deep ocean (see [section 4](#)) and, if this is to be understood, the consequences of wave groups should be examined more closely.

Knowledge of the conclusions that may be drawn from the properties of groups of surface waves raise a number of questions relating to internal waves, for example, how do the zones of extreme values associated with the waves propagate, what is their horizontal and vertical distribution, how are their temporal and spatial properties related, and are they more likely to be observed in measurements at fixed locations than in towed measurements? In the analysis ([section 2](#)) and discussion ([section 3](#) and [4](#)) that follows, we suppose that internal wave groups can exist in the ocean and examine the possible consequences.

## 2. Groups of internal inertial gravity waves

### a. Propagation

It is supposed that there are groups of plane, or two-dimensional long-crested, internal inertial gravity waves in the ocean. We shall suppose that wave groups move as discrete packets or rays of finite length through the water rather than assuming that they are formed simply by the superposition of waves of slightly different frequencies or the modulation of long wave trains. The structure assumed for a group is sketched in [Fig. 2](#). It is elliptical with axes aligned in the directions of group and phase velocity. We consider the associated movement and reoccurrence of the extreme quantities or parameters, which may, for example, be large density perturbations, large wave slopes, high shears, large strains, or low Richardson numbers, as the wave groups propagate. The generic term “breaking” will be used to describe the condition in which a prescribed quantity,  $Q$ , exceeds some specified value within a wave. The *group breaking volume* will be that region of fluid in a group in which  $Q$  exceeds the specified value  $Q_c$  whenever a wave is present within that region. As discussed in [section 3b](#), this will not be synonymous with the region in which the wave is generating, or losing energy to turbulence even, for example, when  $Q_c$  is the critical value of the Richardson number, the value at which a steady laminar stratified shear flow becomes unstable, or even when the specified value is that at which turbulence sets in within the wave.

For simplicity, the buoyancy frequency is supposed to be a constant  $N$ . The Coriolis frequency is  $f$ , and an *exact* solution for the waves can be found with dispersion relation

$$\sigma^2 = (N^2 k^2 + f^2 m^2)/(k^2 + m^2), (1)$$

where  $(k, m)$  is the wavenumber vector of the wave in the  $x, z$  coordinates and  $\sigma$  is the wave frequency ([Gill 1982](#), section 8.4). If

$$\mathbf{c} = \{\sigma/K\}[\sin\theta, -\cos\theta] (2)$$

represents the phase vector of the waves, then the group velocity  $\mathbf{c}_g = (\partial\sigma/\partial k, \partial\sigma/\partial m)$  is found to be

$$\mathbf{c}_g = \{(N^2 - f^2) \sin\theta \cos\theta / K\sigma\}[\cos\theta, \sin\theta]. (3)$$

Here  $K = [k^2 + m^2]^{1/2}$  is the wavenumber and  $\lambda = 2\pi/K$  is the wavelength. If  $0 < \theta < \pi/2$ , this solution corresponds to an upward propagating group of waves traveling at angle  $\theta$  to the horizontal with  $k = K \sin\theta$ ,  $m = K \cos\theta$  and might, for example, represent internal waves generated by flow over bottom topography (see [Bell 1975](#)). The group velocity is parallel to the wave crests and therefore normal to the direction of phase advance, the latter at an angle  $(\pi/2 - \theta)$  below the horizontal; the vector product,  $\mathbf{c} \cdot \mathbf{c}_g$ , is zero. Since (1) and the  $k$ - $m$  and  $K$ - $\theta$  relations give

$$\sigma^2 = N^2 \sin^2\theta + f^2 \cos^2\theta, (4)$$

near-inertial waves with  $\sigma$  near  $f$  have near-horizontal group velocity, with  $\theta$  near zero. If  $\chi = 1 + f^2/(N^2 \tan^2\theta)$ , then  $\sigma^2 = \chi N^2 \sin^2\theta$ .

Since (1) is exact, the phase speed does not change with wave amplitude and, as for surface gravity waves in section 1, it is again assumed that the wave phase speed is constant and, in particular, does not change as the waves pass through a group.

### b. Groups passing fixed points

It is instructive to begin by considering the relation between the number,  $n$ , of waves in a wave group and the number,  $n_r$ , which would be recorded as the group passes a fixed point positioned in the ray path along which the group is propagating. If the width of the group is  $W$  (see [Fig. 2](#)), then  $n \approx W/\lambda$ . The time taken for the group to pass the fixed point is  $L/c_g$ , where  $L$  is the length of the group in the direction of its group velocity  $\mathbf{c}_g$ , so the number of waves recorded as the group passes is  $n_r \approx L/c_g T$ , where  $T$  is the wave period. The ratio  $n_r/n \approx (L/W)(c/c_g)$  since  $\mathbf{c} = \lambda/T$ . Substituting from (1) and (3),  $n_r/n \approx (L/W)\chi \tan\theta/(1 - f^2/N^2)$ , or  $(L/W)\tan\theta$  if  $f \ll N$ . The number of waves recorded depends on the aspect ratio  $L/W$  of the group and the propagation direction  $\theta$ , or, by (4), the wave frequency  $\sigma$ . In general,  $n_r$  will not be equal to  $n$ .



### c. Propagation and repetition of extreme values

Some of the breaking properties of internal wave groups have already been examined (Thorpe 1988). The path of the wave group is prescribed by the group velocity and defines the movement of the region in which the waves are present. Within this region is the group breaking volume  $V$  in which “breaking” occurs (Fig. 2);  $V$  is the volume within which  $Q > Q_c$  when waves are present, and the surface of  $V$  is where  $Q = Q_c$ . Breaking ( $Q > Q_c$ ) occurs along the length of lines of constant phase within  $V$  (see Fig. 3 and later discussion). For sake of argument, we suppose that the  $x$ - $z$  section of  $V$  is elliptical, with major and minor semiaxes of length  $A$  and  $B$  orientated in the directions of  $\mathbf{c}_g$  and  $\mathbf{c}$ , respectively, as shown in Fig. 3b. (This ad hoc assumption is discussed in section 3c). Individual waves break as they enter the volume  $V$ , which itself migrates with the wave group. Since the wave group, and therefore  $V$ , moves at right angles to the wave crests, waves enter  $V$ , and commence breaking, at the wave frequency  $\sigma$ . Unlike surface gravity waves in deep water, the interval between the onset of breaking of successive waves is therefore equal to the wave period  $T$ .

The vector  $\mathbf{c}_b$ , which defines the motion of the center of the zone of breaking in individual waves, for example, position  $X$  in Fig. 2, is determined by the advance of the lines of constant wave phase and by the movement along the wave crest of the point at which breaking occurs, the latter determined by the wave group;  $X$  moves with the lines of constant phase at velocity  $\mathbf{c}$  and along the lines of constant phase at velocity  $\mathbf{c}_g$ , hence  $\mathbf{c}_b = \mathbf{c} + \mathbf{c}_g$ . [These results are the particular case of a more general theory in which the parameter  $\mathbf{c} \cdot \mathbf{c}_g / c^2$  determines the breaking interval and the vector  $\mathbf{c}_b$ ; Thorpe (1988).] The inclination of the vector  $\mathbf{c}_b$  to the horizontal is

$$\phi = -\tan^{-1}[f^2 \cot\theta / N^2]. \quad (5)$$

When  $f \ll N$ , as is usually the case in the upper ocean,  $\phi$  is very small unless  $\sigma$  is very close to  $f$ , that is, when the waves are near inertial. For example, if  $\sigma = f(1 + \delta)$ , where  $\delta \ll 1$ , and if  $f \ll N$ , then  $\tan\phi = -(f/N)/(2^{1/2}\delta^{1/2})$ , which is of order unity if  $\delta \approx (f/N)^2/2$ . Unless the wave frequency is very close to inertial, the center of regions of wave breaking will therefore follow paths that are very close to horizontal, even though the wave group and individual waves move vertically through the ocean.

Since the waves grow as they enter a group, the location within a wave of the position at which  $Q = Q_c$  will not remain exactly at constant phase but may move ahead of the constant phase lines as the wave amplitude grows. The location in a wave at which  $Q$  falls below  $Q_c$  may correspondingly fall behind the lines of constant phase. The movement of  $X$  may therefore differ slightly from the lines of constant phase if, for example, the properties of  $Q$  within individual waves are not symmetrical about, say, the wave crest. This effect however adds a complexity to the analysis, which cannot be resolved; the volume of fluid in which breaking ( $Q > Q_c$ ) occurs at any instant will depend on the distribution of wave amplitudes in space and time within the wave group, and this is presently unknown. It is, moreover, an effect that will be small provided the location of  $Q_c$  follows close to a line of constant phase. For simplicity, we shall therefore assume that the region within an individual wave where breaking occurs is narrow in phase or that the width in the direction of the phase velocity is much less than wavelength, and is close to a line of constant phase. The assumption is equivalent to that of redefining the breaking region in an individual wave at any time as the line of constant phase in  $V$  (where  $Q > Q_c$ ), which advances at the wave phase speed from the point at which  $Q$  first equals  $Q_c$  as the wave enters the group breaking volume, as sketched in Fig. 3. If, for example, the parameter  $Q$  is wave amplitude  $a$ , that is, the vertical displacement of isopycnals at the wave crests from their mean position, the *breaking region* will be that swept out by the wave crests when their amplitude exceeds the given critical value.

If  $\tau$  is the duration of breaking or the time for which an individual wave continues to break, then the length of the minor axis is

$$2B = c\tau \quad (6)$$

since  $\tau$  is just the time that it takes for an individual wave to pass through the breaking region at phase speed  $c$ .

Figure 4 sketches the “scars” left by “breaking regions” as individual waves pass through a wave group “breaking volume” that has moved vertically and horizontally through the  $x$ - $z$  plane to its present position marked by dashed lines and marked “ $V$ .” The time between breaking is  $T$ , and the group breaking volume  $V$  moves with the group, so the distance between sites of the onset of breaking in successive waves,  $AC$  in Fig. 4, is  $c_g T$ . The vertical separation between  $A$  and  $B$  is therefore  $c_g T \sin\theta$ , and (using the sine rule in triangle  $ACD$  in Fig. 4), the vertical distance of  $C$  above  $AB$  (or the

length CD) is  $d_z$ , where  $d_z = \mathbf{c}_g T \sin(\theta - \phi)/\cos\phi$ . Using (3) and (5), this can be written

$$d_z = \lambda(1 - f^2/N^2) \sin\theta, (7)$$

where  $\lambda = 2\pi/K$  is the wavelength. Similarly, the horizontal distance between the breaking regions at A and C is  $AC \cos\theta$ , or

$$d_x = \lambda(1 - f^2/N^2) \cos^2\theta/\chi \sin\theta. (8)$$

To a first approximation the length of the loci of the centers of the breaking regions (i.e., X in Fig. 2) is determined by the duration of breaking  $\tau$  and by the speed of the breaking zone  $\mathbf{c}_b$ . The  $x$  component of  $\mathbf{c}_b$  is  $N^2 \sin\theta/K\sigma$ , so the projection onto the horizontal of the line AB marking a breaking zone in Fig. 4 is  $l'_x = N^2\tau \sin\theta/K\sigma$ , which can be written

$$l'_x = \lambda(\tau/T)/(\chi \sin\theta). (9)$$

However, as can be seen in Fig. 4, the movement of the waves through the elliptical volume V describe volumes in space of rather greater horizontal extent than the line AB. The total horizontal extent  $l_x$  of the breaking regions is found by calculating the difference between the maximum and minimum values of the  $x$  coordinates of points of intersection of a line, which is at angle  $\theta$  to the  $x$  axis that advances at speed  $\mathbf{c}$  and represents a wave phase line within the ellipse V, itself moving at velocity  $\mathbf{c}_g$ ;

$$l_x = l'_x [1 + (A/B)^2 \cos^2\theta \sin^2\theta \chi^2]^{1/2}. (10)$$

Similarly, the vertical extent of the breaking region caused by individual breaking waves is

$$l_z = \lambda(\tau/T) \sin\theta [(A/B)^2 + (\chi - 1)^2/(\chi^2 \cos^2\theta)]^{1/2}, (11)$$

using (6).

The scars left by the breaking regions of successive waves overlap in the horizontal if  $l_x > d_x$ , that is, if

$$\tau/T > (1 - f^2/N^2) \cos^2\theta [1 + (A/B)^2 \cos^2\theta \sin^2\theta \chi^2]^{-1/2}. (12)$$

In this case a vertical profile with a microstructure probe would sample at least one region in which breaking had occurred or is still present. Similarly, if breaking regions are to overlap in the vertical, as illustrated in Fig. 4b, so that a horizontal tow would sample at least one region in which breaking had occurred (no gaps as illustrated in Fig. 4a), then  $l_z > d_z$ , or

$$\tau/T > (1 - f^2/N^2) [(A/B)^2 + (\chi - 1)^2/(\chi^2 \cos^2\theta)]^{-1/2}. (13)$$

Finally, for scars to overlap with one another as illustrated in Fig. 4b, the maximum extent of a scar in the direction of  $\mathbf{c}_g$ ,  $2A$ , must exceed  $AC$ ; that is,  $2A > \mathbf{c}_g T$ . This can be written  $A/B > \mathbf{c}_g T/c\tau$  or

$$\tau/T > (\mathbf{c}_g/c)/(A/B). (14)$$

#### d. Groups passing a fixed vertical or horizontal sampling arrays

It is of interest to establish what could be detected as a group of internal waves propagates past a fixed vertical instrumented mooring or a position at which, for example, repeated CTD or microstructure profiles are being taken. Figure 5a shows the elliptical breaking region, V, at a time  $t$  being carried with velocity  $\mathbf{c}_g$  past a fixed vertical line at constant horizontal position,  $x = 0$  (e.g., the horizontal location of the measuring array). The major axis of the ellipse passes through a

fixed point,  $z_0$ , on the vertical line, which does not propagate vertically. [Figure 5b](#) shows the breaking volume and the breaking waves in  $z-t$  space. It is easily shown that the shape of the breaking region here is again elliptical. The vertical dimension of the breaking region at time  $t$  is the length of the intersection of  $V$  with the  $z$  axis shown in [Fig. 5a](#). The constant phase lines of breaking waves propagate downward at speed  $\mathbf{c}_z = -\sigma/m$ , or  $\mathbf{c}_z = -\sigma/(K \cos\theta)$ . [This is not the vertical component of the phase speed  $\mathbf{c}$ , given in (2); lines of constant phase are given by  $kx + mz - \sigma t = \text{const}$  and intersect  $x = 0$  at  $z = (\sigma/m)t + \text{const}$ , where  $m = -K \cos\theta$ .] Lines of constant phase intersect the  $t$  axis ( $z = 0$ ) at the wave period  $T$ . If successive waves break at a fixed depth  $z$ , the interval between breaking is also  $T$ . The breaking region,  $V$ , in [Fig. 5a](#) moves past the vertical line at speed  $\mathbf{c}_{gx} = (N^2 - f^2)\cos^2\theta \sin\theta/K\sigma$ , and its horizontal width is  $l_x$ , so the time taken to pass is  $T_z = l_x/\mathbf{c}_{gx}$  or

$$T_z = \tau[1 + (A/B)^2 \cos^2\theta \sin^2\theta \chi^2]^{1/2} \div \{\cos^2\theta[1 - (f/N)^2]\}. \quad (15)$$

The maximum  $z$  at which  $V$  and the vertical line,  $x = 0$ , intersect is at  $z - z_0 = B/\cos\theta$ , so the vertical scale of the breaking region is  $L_z = 2B/\cos\theta = c\tau/\cos\theta$  using (6), or

$$L_z = \lambda(\tau/T)/\cos\theta, \quad (16)$$

since  $\mathbf{c} = \lambda/T$ . Simultaneous breaking of waves may occur at two levels if the duration of breaking (the period for which the waves shown in [Fig. 5b](#) “break,” exceeds  $T$ ). The maximum duration is given by  $L_z$  divided by absolute value of the speed of the constant phase lines,  $\mathbf{c}_z$ ; that is,  $c\tau/\cos\theta/(K \cos\theta/\sigma) = \tau$ . A necessary condition for breaking to occur simultaneously at two levels is  $\tau > T$ . The number of waves that will be observed to break as the group passes is approximately  $T_z/T + 1$ .

The corresponding times and lengths as  $V$  is carried upward through a horizontal line or array of instruments are

$$T_x = \chi\tau[1 + A^2 \tan^2\theta/B^2]^{1/2}/(1 - f^2/N^2) \quad (17)$$

and

$$L_x = \lambda(\tau/T)/\sin\theta. \quad (18)$$

### 3. Discussion

#### a. Recurrence of extreme events

The discussion in [section 2](#) has implications for the measurement of extreme events in internal waves. The number of waves observed as a group passes a fixed measurement point. Compared to the number in a group,  $n_r/n$  is approximately equal to  $(L/W)(\mathbf{c}/\mathbf{c}_g)$  ([section 2b](#)) and therefore depends on the group aspect ratio  $L/W$ . The conditions for sampling breaking in vertical profiles (12), horizontal profiles (13), or for groups to produce a continuous scar zone in which breaking has occurred (14) all depend on the generally unknown aspect ratio  $A/B$  of the group breaking volume,  $V$  (or on its eccentricity,  $e = [1 - B^2/A^2]^{1/2}$ ).

In the [Mowbray and Rarity \(1967\)](#) laboratory experiments, an oscillating cylinder produced groups containing some two waves. With this in mind, it is plausible to think of a wave group having an extent in direction  $\mathbf{c}_g$  equal to the product of  $\mathbf{c}_g$  and the period during which waves in the group are generated  $T_g$ , and a dimension in the  $\mathbf{c}$  direction  $n\lambda$ , where  $n$  is the number of waves in the group produced by the wave generator. If we now suppose that the areas of the group and the group breaking volume  $V$  have similar aspect ratios, then  $L/W \approx A/B = T_g \mathbf{c}_g/n\lambda = (n_g/n)(\mathbf{c}_g/\mathbf{c})$ , where  $n_g = T_g/T$  is the number of wave periods for which the forcing of the waves in the group continues. From [section 2b](#) it follows that  $n_r = n_g$ ; the number of waves recorded as the group passes a fixed point is equal to the number generated in a fixed location. In the laboratory experiments,  $n_g$  was usually long to achieve near-steady conditions, but in the ocean forcing is generally transient. Tidal forcing varies over the spring–neap tides or with a timescale of some 14 days so that  $n_g$  may be of order 20. With

localized forcing (e.g., at the shelf breaking or at an isolated ridge),  $n$  will be much smaller, of order 1–3 [e.g., see [Pingree and New's \(1989\)](#) observations]. Now  $c_g/c = \{[1 - (f/\sigma)^2][(N/\sigma)^2 - 1]\}^{1/2}$  tends to zero as  $\sigma$  tends to  $f$ . For the  $M_2$  tide ( $\sigma = 1.4 \times 10^{-4} \text{ s}^{-1}$ ) at  $45^\circ$  latitude ( $f = 1.03 \times 10^{-4} \text{ s}^{-1}$ ) and when  $N = 10^{-3} \text{ s}^{-1}$ , we find  $\theta$  is equal to  $5.5^\circ$  and  $c_g/c \approx 4.8$ , so  $A/B$  may be of order 40. For *near-inertial waves* the aspect ratio is even less certain. Inertial wave forcing by storms ([Pollard 1970](#)) may continue for say, 0.5–3 days, or 1–5 wave periods, and, given that the number of waves observed is 3–7, this suggests that  $n/n_g$  may be of order unity. If  $1.001f < \sigma < 1.01f$  at  $45^\circ$  latitude and  $N = 10^{-3} \text{ s}^{-1}$ , then  $0.26^\circ < \theta < 0.84^\circ$  and  $1.34 > c_g/c > 0.43$ . It follows that, unless  $\sigma$  is very close to  $f$ ,  $c_g/c$  is of order unity, and consequently  $A/B$  may be of order unity. Observational evidence, however, suggests that the horizontal extent (proportional to  $A$  since  $\theta \ll 1$ ) of inertial wave packets may be tens of kilometers in extent while their vertical (proportional to  $B$ ) extent is of order 1 km or less ([Marmorino et al. 1987](#)), so  $A/B \approx 10$ –20. The assumption of a localized source, as in the Mowbray and Rarity experiments, is most probably in error; storms move during inertial waves generation, leaving a wake of inertial waves. A third class of waves in which a group structure may be apparent are those generated as *internal lee waves* by oscillating tidal flow over small horizontal scale (1–3 km) topography ([Bell 1975](#); [Thorpe 1996](#)). For example, internal waves may be generated during part of a tidal cycle when the flow  $\mathbf{v}$  along a continental slope with inclination  $\alpha$  to the horizontal lies in the range

$$\begin{aligned} N/\{l[\sin^2\alpha \cos^2\beta(1 - f^2/N^2)^2 + f^2/N^2]^{1/2}\} \\ < \mathbf{v} < N/(l \sin\beta), \end{aligned} \quad (19)$$

where  $l$  is the wavenumber of the topographic roughness and  $\beta$  is the angle between the topography and the downslope direction. Typically, 2–5 internal gravity waves may be generated over the period of a few hours when (19) is satisfied, with  $A/B \approx 1$  and  $\theta$  in the range  $5^\circ$ – $20^\circ$ .

[Table 1](#) shows values of  $\theta$ ,  $\chi$ ,  $A/B$ , and  $\phi$  for these inertial, tidal, and lee waves, as well as the ratio  $n_r/n$ , the number of waves recorded as a group passes a fixed observation point divided by the number of waves in the group, and the values that must be exceeded by  $\tau/T$  for (12), (13), and (14) to be satisfied. The inclination of the breaking vector to the horizontal for near-inertial waves is large and sensitive to the precise value of  $\sigma/f$ . Far more waves than exist in a group will be recorded at a fixed point if inertial or tidal waves propagate past it, but the number of waves  $n$  in lee wave groups may be undersampled by point measurements. Extreme values persisting in inertial or tidal waves for times  $>0.15T$  will result in observations of simultaneous layers overlying one another in the vertical (12), at least one being encountered in horizontal sections through the group (13), and regions in which given values has been exceeded as a group passes are generally connected to each other (14), favoring rather uniform mixing if  $Q_c$  is the breaking condition. Lee wave groups require extrema to persist for more than a wave period (i.e.,  $\tau > T$ ) for detection always to be found in vertical (12) or horizontal (13) sections, while  $\tau$  must be significantly greater than  $T$  if fluid regions in which extrema have been reached are to be connected to one another. Here turbulence, if it occurs, is more patchy, with isolated layers.

### b. Wave breaking

Here  $Q_c$  has been defined as a value of some parameter that is exceeded within the group breaking volume  $V$ . It might, for example, be some value of shear. Groups of larger-scale internal waves moving through a background or ambient field of shorter waves may enhance the local shear, or modify the density field, in such a way that the shorter waves themselves break ([Thorpe 1989](#)). The zones and scars left by such breaking are identical to those within which  $Q$  exceeds  $Q_c$ , provided that the small-scale wave spectrum is initially isotropic (i.e., before the arrival of the larger-scale wave group) and not patchy on the scale of the larger waves.

Even when  $Q_c$  characterizes the condition for the onset of instability in an internal wave, care is needed in identifying the regions in which  $Q_c$  is exceeded with those in which turbulence may be found. Turbulence does not set in immediately. Small disturbances first undergo amplification before overturning, and in an unsteady flow turbulence may well set in when the threshold parameter is significantly greater than critical. In a steady flow turbulence resulting from Kelvin–Helmholtz instability persists for a time from its generation until its decay (in a turbulent–laminar transition) of about  $24N^{-1}$ , where  $N$  is the local buoyancy frequency, or about 4 buoyancy periods ([Thorpe 1973](#)). This is longer than the duration of “puffs” estimated by [Gregg et al. \(1986\)](#), suggesting that their source may not be Kelvin–Helmholtz instability but perhaps convective overturn (more likely in waves with frequency  $\sigma$  well above  $f$ ; [Thorpe 1999](#), manuscript submitted to *J. Phys. Oceanogr.*). The region,  $V$ , defined as the breaking region may identify the location and time in which turbulence will set in, but turbulence may persist after  $V$  has passed, just as foam or turbulence may persist after the passage of a breaking wave crest over the sea surface. Turbulence may be maintained in a local region by successive waves of a group breaking there provided the turbulence generated by the first continues until the second arrives. If Kelvin–Helmholtz instability is the source,



the time interval,  $24N^{-1}$ , and the period of recurrence of breaking,  $T$ , implies that internal waves with  $\sigma/N < 0.25$  (e.g.,  $\theta < 13.3^\circ$ , if  $f/N = 0.1$ ) will not generate turbulence that is sustained from one wave until the next unless a further source of energy is available, for example, shorter waves which surrender their energy on meeting the turbulent patch. It should not, however, be assumed that turbulence generated by the breaking of internal waves will be limited in scale to one wave; although the breaking of surface waves is usually associated with instability and foam occurring at or near the crest of one wave, it is conceivable (though unlikely; Thorpe 1999, manuscript submitted to *J. Phys. Oceanogr.*) that several waves may take part “collectively” in internal wave breaking. The “scars” left by single waves will then underestimate the zone of turbulence.

### c. The shape of the breaking region $V$

It has been assumed that  $V$  is elliptical with axes parallel to  $\mathbf{c}_g$  and  $\mathbf{c}$ . This is a special case since the central point of individual waves crossing  $V$  move along the semimajor axis. This is not so for ellipses with other orientations. If, for example, the axes are horizontal, the central point of individual waves crossing  $V$  move along a trajectory *through* the ellipse (i.e., relative to the ellipse, which itself moves with speed  $\mathbf{c}_g$ ) between the points at which waves enter and leave it. This is a straight line joining points at which lines of slope  $\theta$  touch the ellipse. Their inclination to the horizontal is  $\gamma \equiv \tan^{-1} [(-B^2/A^2) \cot\theta]$ . The new inclination of the breaking vector  $\mathbf{c}_b$  to the horizontal,  $\phi_1$ , now depends on the aspect ratio of  $V$  and is given by  $\tan\phi_1 = [(\mathbf{c}_g/\mathbf{c}) \sin\theta \sin(\theta + \gamma) - \sin\gamma]/[(\mathbf{c}_g/\mathbf{c}) \cos\theta \sin(\theta + \gamma) + \cos\gamma]$ . Corresponding values are given in [Table 1](#). They are identical to  $\phi$  when  $V$  is circular, that is, when  $A = B$ , and less negative for near-inertial waves.

## 4. Conclusions

Breaking surface waves generate an intermittently produced, but continuously maintained, layer of turbulence at the sea surface, provided that the mean interval between breaking waves passing a fixed position is sufficiently short and the turbulence sufficiently long-lived ([Thorpe 1995](#)). In mid water in the deep ocean there is little evidence turbulence is often, if ever, sustained. For example, [Gregg et al. \(1986\)](#) find turbulent patches in the California Current cover 8%–36% of the water column, the percentage depending on the threshold level used. Dissipation is consequently low. Mixing is particularly weak over midlatitude plains ([Kunze and Sanford 1996](#)), although it may be larger near islands ([Osborn 1978](#)). Recent observations in the Brazil Basin ([Polzin et al. 1997](#)), however, show that higher dissipation does occur over areas of rough topography, there the Mid-Atlantic Ridge, and that levels of diapycnal diffusion much exceeding molecular are then found almost throughout the water column. It appears possible that internal waves generated by tidal flow over the rough ridge topography, either as baroclinic tides or as higher-frequency lee waves (see [section 3](#)), are the energy source for the enhanced mixing (W. Munk 1997, personal communication), but little direct information is yet available of the nature of the propagating waves or the intermittency of the events leading to the onset of turbulence.

The discussion in [section 3a](#) shows that internal tides are more likely to result in more general mixing with connected regions of extreme values or breaking with less patchiness than lee waves at the same  $\tau/T$  values. Turbulence generated by Kelvin–Helmholtz instability is, however, unlikely to be maintained from one breaking wave to the next ([section 3b](#)). The theory offers an explanation of the difference between the persistent patches of turbulence observed in near-inertial waves and puffs in internal gravity waves observed by [Gregg et al. \(1986\)](#) and the spatial variations in turbulent patch structure, particularly the upward vertical migration since  $\phi$  is negative, of the patches of turbulence in inertial waves propagating with a downward component of group velocity from the sea surface. Wave groups may also help explain the vertical migration of low-density lenses observed by [Pinkel et al. \(1991\)](#). Perhaps these are “extreme values,” here of the distortion to the density field associated with wave groups?

Our interest in the relation between internal wave groups and mixing, or the generation of extreme values, was rekindled by observations of layers of nearly uniform density and with typical vertical and horizontal scales of 0.5 and 1 km, respectively, in the relatively uniformly stratified water underlying the seasonal thermocline, and over the sloping bottom, at the sides of Lake Geneva ([Thorpe and Lemmin 1998](#)). The observations made from a small submarine in summer 1997 suggested that the layers, which were often isolated single layers, might be a consequence of breaking, or nearly breaking, internal waves, amplified in reflection from a sloping bottom. We found their isolation intriguing. Could they be explained as a consequence of the low-frequency, subcritical, wave reflection of internal wave groups? The answer from [Table 1](#) appears to be “yes,” provided the waves have properties similar to those described here as lee waves. It is likely that near-breaking conditions are sustained for times  $\tau$ , shorter than the period  $T$  of the waves, so that only one layer of extreme values will be produced and observed.

The results emphasize the importance of the ratio  $\tau/T$  and that, unless “breaking” or the extreme values is maintained for periods of time which approach the wave period, the consequent patches of breaking will be disconnected and separated in space and time. The analysis demonstrates the importance of some poorly known properties of internal gravity waves that deserve further study, particularly the existence of groups and the size and shape of regions of extreme values.

I am grateful to an unknown reviewer for drawing my attention to the sensitivity of some of the conclusions to the orientation assumed for the group breaking volume V.

---

## REFERENCES

- Apel, J. R., J. R. Holbrook, A. K. Liu, and J. J. Tsai, 1985: The Sulu Sea internal soliton experiment. *J. Phys. Oceanogr.*, **15**, 1625–1651.. [Find this article online](#)
- Bell, T. H., 1975: Topographically generated internal waves in the open ocean. *J. Geophys. Res.*, **80**, 320–327..
- Benjamin, T. B., 1967: Instability of periodic wavetrains in nonlinear dispersive systems. *Proc. Roy. Soc. London A*, **299**, 59–75..
- Borisenko, Yu. D., K. Y. Voronovich, A. I. Leonov, and Yu. Z. Miropolskiy, 1976: Towards a theory of non-stationary weakly nonlinear internal waves in the stratified ocean. *Atmos. Ocean Phys.*, **12**, 174–179..
- Brekhovskikh, L. M., K. V. Konjarv, K. D. Sabinin, and A. N. Serikov, 1975: Short-period internal waves in the sea. *J. Geophys. Res.*, **80**, 856–864..
- Broutman, D., and R. Grimshaw, 1988: The energetics of the interaction between short small-amplitude internal waves with near-inertial waves. *J. Fluid Mech.*, **196**, 93–106..
- Desaubies, Y., and W. K. Smith 1982: Statistics of Richardson number and instability in oceanic internal waves. *J. Phys. Oceanogr.*, **12**, 1245–1259.. [Find this article online](#)
- Donelan, M., M. S. Longuet-Higgins, and J. S. Turner 1972: Periodicity in whitecaps. *Nature*, **239**, 255–261..
- Dushaw, B. D., B. D. Cornuelle, P. F. Worster, B. M. Howe, and D. S. Luther, 1995: Barotropic and baroclinic tides in the central North Pacific determined from long-range reciprocal acoustic transmission. *J. Phys. Oceanogr.*, **25**, 631–647.. [Find this article online](#)
- Eriksen, C. C., 1978: Measurements and models of finestructure, internal gravity waves, and wave breaking in the deep ocean. *J. Geophys. Res.*, **83**, 2989–3009..
- Evans, D. L., 1982: Observations of small scale shear and density structure in the ocean. *Deep-Sea Res.*, **29**, 581–595..
- Fedorov, K. N., and A. I. Ginsberg, 1986: Visually observed sea surface phenomena. *Oceanology*, **26**, 1–7..
- Farmer, D. M., and S. Vagel, 1988: On the determination of breaking surface wave distributions using ambient sound. *J. Geophys. Res.*, **93**, 3591–3600..
- Garrett, C., and W. Munk, 1972: Oceanic mixing by breaking internal waves. *Deep-Sea Res.*, **19**, 823–832..
- , and —, 1975: Space-time scales of internal waves: A progress report. *J. Geophys. Res.*, **80**, 291–297..
- Gill, A. E., 1982: *Atmosphere–Ocean Dynamics*. Academic Press, 662 pp..
- Gregg, M. C., E. A. D’Asaro, T. J. Shay, and N. Larson, 1986: Observations of persistent mixing and near-inertial internal waves. *J. Phys. Oceanogr.*, **16**, 856–885.. [Find this article online](#)
- Hasselmann, K., 1962: On the non-linear energy transfer in a gravity wave spectrum. *J. Fluid Mech.*, **12**, 481–500..
- Henye, F. S., and N. Pomphrey, 1983: Eikonal description of internal-wave interactions. A non-diffusive picture of “induced diffusion”. *Dyn. Atmos. Oceans*, **7**, 189–208..
- Käse, R. H., and G. Siedler, 1980: Internal wave kinematics in the upper tropical Atlantic. *Deep-Sea Res.*, **26**, 161–189..
- Kunze, E., and T. B. Sanford, 1996: Abyssal mixing: Where it is not. *J. Phys. Oceanogr.*, **26**, 2286–2296.. [Find this article online](#)
- , A. J. Williams, and M. G. Briscoe, 1990: Observations of shear and vertical stability from a neutrally buoyant float. *J. Geophys. Res.*, **98**, 127–142..

- Leaman, K. D., and T. B. Sanford, 1975: Vertical energy propagation of inertial waves: A vector spectral analysis of velocity profiles. *J. Geophys. Res.*, **80**, 1975–1978..
- Levine, M. D., C. A. Paulson, M. G. Briscoe, R. A. Weller, and H. Peters, 1983: Internal waves in JASIN. *Philos. Trans Roy. Soc. London A*, **308**, 389–405..
- Longuet-Higgins, M. S., 1962: Resonant interaction between two trains of gravity waves. *J. Fluid Mech.*, **12**, 321–332..
- ↵1975: Integral properties of periodic gravity waves of finite amplitude. *Proc. Roy. Soc. London A*, **342**, 157–174..
- ↵1986: Wave group statistics. *Oceanic Whitecaps*, E. C. Monahan and G. MacNiocaill, Eds., D. Reidel, 15–35..
- Marmorino, G. O., 1987: Observations of small-scale mixing processes in the seasonal thermocline. Part II: Wave breaking. *J. Phys. Oceanogr.*, **17**, 1348–1355.. [Find this article online](#)
- ↵L. J. Rosenblum, and C. L. Trump, 1987: Fine-scale temperature variability: The influence of near-inertial waves. *J. Geophys. Res.*, **92**, 13 049–13 062..
- Martin, S., W. Simmons, and C. Wunsch, 1972: The excitation of resonant triads by single internal waves. *J. Fluid Mech.*, **53**, 17–44..
- Mied, R. P., G. L. Lindemann, and C. L. Trump, 1987: Inertial wave dynamics in the North Atlantic subtropical zone. *J. Geophys. Res.*, **92**, 13 065–13 074..
- Mowbray, D. E., and B. S. H. Rarity, 1967: A theoretical and experimental investigation of the phase configuration of internal waves of small amplitude in a density stratified fluid. *J. Fluid Mech.*, **28**, 1–16..
- Munk, W., 1966: Abyssal recipes. *Deep-Sea Res.*, **13**, 707–730..
- ↵1981: Internal waves and small scale processes. *Evolution of Physical Oceanography*, B. Warren and C. Wunsch, Eds., The MIT Press, 236–263..
- New, A. L., 1988: Internal tidal mixing in the Bay of Biscay. *Deep-Sea Res.*, **35**, 691–709..
- ↵and R. D. Pingree, 1990: Large amplitude internal soliton wave packets in the Bay of Biscay. *Deep-Sea Res.*, **37**, 513–524..
- ↵and — ↵1992: Local generation of internal soliton packets in the central Bay of Biscay. *Deep-Sea Res.*, **39**, 1521–1534..
- Osborn, T. R., 1978: Measurements of energy dissipation adjacent to an island. *J. Geophys. Res.*, **83**, 2939–2957..
- Ostrovski, L. A., and Yu. A. Stepanyants, 1989: Do internal solitons exist in the ocean? *Rev. Geophys.*, **27**, 293–310..
- Padman, L., and I. S. F. Jones, 1985: Richardson number statistics in the seasonal thermocline. *J. Phys. Oceanogr.*, **15**, 844–854.. [Find this article online](#)
- Phillips, O. M., 1960: On the dynamics of unsteady gravity waves of finite amplitude. *J. Fluid Mech.*, **9**, 193–217..
- ↵1966: *The Dynamics of the Upper Ocean*. Cambridge University Press, 261 pp..
- Pingree, R. D., and A. L. New, 1989: Downward propagation of internal tidal energy into the Bay of Biscay. *Deep-Sea Res.*, **36**, 735–758..
- Pinkel, R., 1983: Doppler sonar observations of internal waves: Wave-field structure. *J. Phys. Oceanogr.*, **13**, 804–815.. [Find this article online](#)
- ↵J. Sherman, J. Smith, and S. Anderson, 1991: Strain: Observations of the vertical gradient of isopycnal vertical displacement. *J. Phys. Oceanogr.*, **21**, 527–540.. [Find this article online](#)
- Pollard, R. T., 1970: On the generation by winds of inertial waves in the ocean. *Deep-Sea Res.*, **17**, 795–812..
- ↵and R. C. Millard, 1970: Comparison between observed and simulated wind-generated inertial oscillations. *Deep-Sea Res.*, **17**, 813–821..
- Polzin, K. L., J. M. Toole, J. R. Ledwell, and R. W. Schmitt, 1997: Spatial variability of turbulent mixing in the abyssal ocean. *Science*, **276**, 93–96..
- Ray, R. D., and G. T. Mitchum, 1996: Surface manifestations of internal tides generated near Hawaii. *Geophys. Res. Lett.*, **23**, 2101–2104..
- Sabinin, K. D., 1973: Certain features of short period internal waves in the ocean. *Atmos. Oceanic Phys.*, **9**, 32–36..

Simpson, J. H., 1972: A free-fall probe for the measurement of velocity microstructure. *Deep-Sea Res.*, **19**, 331–336..

Smyth, W. D., D. Hebert, and J. N. Moum, 1996: Local ocean response to a multiphase westerly wind burst. Part I: Dynamic response. *J. Geophys. Res.*, **101**, 22 495–22 512..

Thorpe, S. A., 1973: Experiments on instability and turbulence in a stratified shear flow. *J. Fluid Mech.*, **61**, 731–751..

— , 1974: The excitation, dissipation, and interaction of internal waves in the deep ocean. *J. Geophys. Res.*, **80**, 328–338..

— , 1977: On the stability of internal wavetrains. *A Voyage of Discovery*, M. Angel, Ed., Pergamon, 199–212..

— , 1988: A note on breaking waves. *Proc. Roy. Soc. London A*, **419**, 323–335..

— , 1989: The distortion of short internal waves produced by a long wave, with application to ocean boundary mixing. *J. Fluid Mech.*, **208**, 395–415..

— , 1995: Dynamical processes of transfer at the sea surface. *Progress in Oceanography*, Vol. 35, Pergamon, 315–352..

— , 1996: The cross-slope transport of momentum by internal waves generated by along-slope currents over topography. *J. Phys. Oceanogr.*, **26**, 191–204.. [Find this article online](#)

— , and P. N. Humphries, 1980: Bubbles and breaking waves. *Nature*, **283**, 463–465..

— , and U. Lemmin, 1998: Investigating the thermal structure of Lake Geneva using a submarine. *Eos, Trans. Amer. Geophys. Union*, **79** (1), p. OS41..

Trulsen, K., 1989: Crest pairing by modulation theory. *J. Geophys. Res.*, **103**, 3143–3147..

Winters, K. B., and E. A. D’Asaro, 1992: Two-dimensional instability of finite amplitude internal gravity wave packets near a critical level. *J. Geophys. Res.*, **94**, 12 709–12 719..

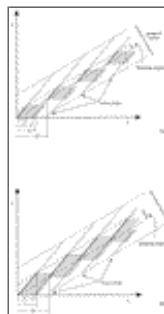
## Tables

Table 1. Values of the inclination of the wave group propagation direction to horizontal,  $\theta$ ;  $\chi [= \sigma^2/(N^2 \sin^2\theta)]$ ; the aspect ratio,  $A/B$  of breaking volume;  $V$  the inclination of the wave breaking vector  $\mathbf{c}_b$ ; first ( $\phi$ ) when the axes of  $V$  are parallel to  $\mathbf{c}_g$  and  $\mathbf{c}$  and second ( $\phi_1$ ) when they are horizontal and vertical (see section 3c); ratio of group speed to phase speed  $c_g/c$ ; ratio of the number of waves recorded as a group passes a fixed observation point to the number of waves in the group  $n_r/n$ ; and the values that must be exceeded by  $\tau/T$  for (12), (13), and (14) to be satisfied, respectively, all when  $f/N = 0.103$ .

	$\theta$	$\chi$	$A/B$	$\phi$	$\phi_1$	$c_g/c$	$n_r/n$	(12)	(13)	(14)
Internal waves	0.26	515	10	-66.8	-61.3	0.42	23.6	0.042	0.098	0.010
	0.26	515	20	-66.8	-24.0	0.42	47.6	0.021	0.049	0.021
	0.84	50.3	10	-35.9	-19.1	1.34	7.4	0.020	0.099	0.13
$M_2$ tide	5.87	2.16	40	-6.3	1.5	4.79	8.3	0.025	0.025	0.12
	5.0	2.39	1	-0.1	-0.1	4.74	0.2	0.95	0.85	4.7
Internal tide waves	20.0	1.08	1	-1.7	-1.7	2.52	0.4	0.82	0.98	2.5

Click on thumbnail for full-sized image.

## Figures



Click on thumbnail for full-sized image.

Fig. 1. The propagation of surface gravity waves in a wave group and their breaking. For simplicity, a steady state is assumed

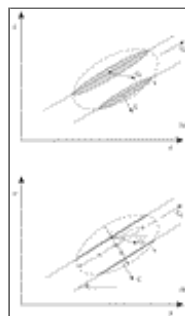


in which the wave group continues to contain breaking waves indefinitely and there is no mean flow. The full lines shows the positions of waves propagating in the  $x$  direction as a function of time  $t$ , beginning or ending as they enter or leave the group marked by dotted lines. The slope of the full lines is  $c$ , the wave phase speed. The group propagates at the group speed  $c_g$  (the slope of the dotted lines), also in direction  $x$ , and for surface waves in deep water,  $c_g = c/2$ . The dashed lines, moving forward with the wave group, show the location of the region of breaking (or extreme) waves, marked as bold lines within the group. The speckled regions show the location of foam left by the breaking waves. In (a) the duration of breaking  $\tau < T$ , and the foam patches persist for a time  $T_f$  less than  $2T - \tau$ . The patches of foam produced by successive waves do not overlap in space or time. In (b),  $2T > \tau > T$ , and  $\tau \approx T_f$ . Here there are times,  $2T - \tau$  long, when no waves break, but at least one wave breaks at any position  $x$  as the group passes. Photographs might show no wave breaking, but a fixed wave-breaking detector would record at least one breaking wave. Foam patches overlap in both space and time. If  $T_f$  were less than  $2t - \tau$ , foam patches would overlap in space but not in time.



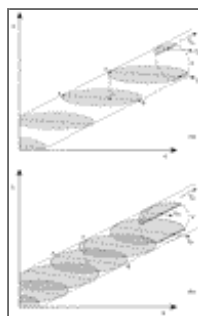
[Click on thumbnail for full-sized image.](#)

Fig. 2. An internal wave group of dimensions  $W$  and  $L$  lies within the section marked by the dotted line at a fixed time  $t$  and moves with velocity  $c_g$  along a ray path in  $x$ - $y$  space. Lines of constant wave phase are marked by full lines and advance with velocity  $c$ . The breaking region  $V$  is marked by the dashed contour. Within  $V$  some quantity  $Q$  associated with the wave field will exceed some specified value  $Q_c$  as the waves pass through. Sections  $AA$  and  $BB$  show the amplitude of  $Q$  in directions normal to and along the lines of constant phase, respectively. The value  $Q_c$  is exceeded only in regions surrounding the bold lines of constant phase in  $V$ . The point  $X$  at the center of a line of constant phase within  $V$  moves with velocity  $c_b = c + c_g$ .



[Click on thumbnail for full-sized image.](#)

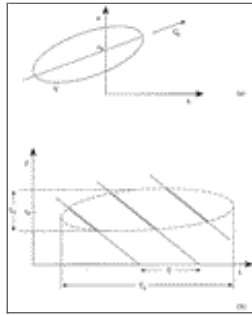
Fig. 3. (a) Instantaneous regions of “breaking,”  $Q > Q_c$ , within the internal waves lying within the group breaking region  $V$ . The width of the regions is determined by the shape of the waves within volume  $V$  of the wave group. (b) The constant phase lines marking the center of the “breaking” regions. The vector  $c_b$  indicates the velocity of advance of the breaking zone and is in a direction  $\phi$  above the horizontal. It is assumed that  $V$  is elliptical with semimajor and minor axes  $A$  and  $B$ , respectively, as shown.



[Click on thumbnail for full-sized image.](#)

Fig. 4. The “breaking regions” produced by a wave group that has moved through the  $x$ - $z$  plane drawn at time  $t$ . These regions will not be “active.” Only in the limited volume of the wave group breaking volume  $V$  will the specific value of  $Q$  exceed  $Q_c$  at the time  $t$  (see Fig. 2). The dotted lines show the region swept out by the group breaking volume  $V$ . Stippled areas mark the volumes within which waves have broken (i.e., where  $Q$  was greater than  $Q_c$ ) as they passed through  $V$ . Here  $A$  and  $C$  mark the

points at which successive waves enter the volume  $V$  and  $B$  is the point where the wave, entering at  $A$ , leaves  $V$ . In (a) the regions in which breaking has occurred do not overlap in space. In (b) regions overlap in space. In both cases illustrated, two waves break simultaneously. In (a) there are positions  $z$  between the breaking waves where no breaking occurs at time  $t$ , although there are no such positions in  $x$ ; the possibility of a horizontal towed section through  $V$  detecting “breaking” is less than that of a vertical free-fall profiler.



[Click on thumbnail for full-sized image.](#)

Fig. 5. (a) The propagation of the breaking volume past a fixed vertical line at  $x = 0$ . The major axis of the elliptical section of  $V$  moves through the point  $z = z_0$ . (b) The dashed line shows the position of  $V$  in the  $t-z$  frame of reference. The lines represent lines of constant phase moving downward and “breaking” (shown by thicker lines) within  $V$ .

*Corresponding author address:* Dr. S. A. Thorpe, Department of Oceanography, University of Southampton, Southampton Oceanography Centre, European Way, Southampton S014 3ZH, United Kingdom.

E-mail: [sxt@mail.soc.soton.ac.uk](mailto:sxt@mail.soc.soton.ac.uk)

[top ▲](#)



© 2008 American Meteorological Society [Privacy Policy and Disclaimer](#)  
 Headquarters: 45 Beacon Street Boston, MA 02108-3693  
 DC Office: 1120 G Street, NW, Suite 800 Washington DC, 20005-3826  
[amsinfo@ametsoc.org](mailto:amsinfo@ametsoc.org) Phone: 617-227-2425 Fax: 617-742-8718  
[Allen Press, Inc.](#) assists in the online publication of *AMS* journals.